*Transactions of the Korean Nuclear Society Autumn Meeting*
*Yeosu, Korea, October 25-26, 2018*

# Development of Mesh-type Computational Phantoms for Reference Korean Adults

Chansoo Choi [a], Thang Tat Nguyen [b], Yeon Soo Yeom [c], Hanjin Lee [a], Haegin Han [a], Bangho Shin [a], Xujia Zhang [a], Chan Hyeong Kim [a*]

[a]*Department of Nuclear Engineering, Hanyang University, 222 Wangsimni-ro, Seongdong-gu, Seoul 04763, Korea*
[b]*School of Nuclear Engineering and Environmental Physics, Hanoi University of Science and Technology, 1 Dai Co Viet road, Hai Ba Trung distric, Hanoi, Vietnam*
[c]*National Cancer Institute, National Institute of Health, 9609 Medical Center Drive, Bethesda, MD 20850, USA*
[*]*Corresponding author: chkim@hanyang.ac.kr*

## 1. Introduction

Previously, Korean adult male and female voxel-type reference computational phantoms, called HDRK-Man [1] and HDRK-Woman [2], were developed for use in dose calculations for radiological protection purpose of Korean adults. However, the voxel-type reference Korean phantoms due to the limited voxel resolutions (male: $1.981 \times 1.981 \times 2.0854$ mm$^3$ and female: $2.0351 \times 2.0351 \times 2.0747$ mm$^3$) do not properly represent thin or small structures such as micron-scale radiosensitive target and source regions in alimentary and respiratory tract systems, skin, urinary bladder, and eye lens, eventually leading to unreliable dose calculations. The voxel phantoms were constructed based on the outdated reference Korean data [3] while new reference Korean data [4] have been established. Moreover, due to the nature of the voxel geometry, it is difficult to deform the voxel-type phantoms into different body sizes or postures to extend their applications to individualized dose calculations from medical, accidental or emergency exposures.

In the present study, we developed new mesh-type reference Korean phantoms (MRKPs) based on the same phantom construction techniques used for the recently developed mesh-type ICRP reference computational phantoms (MRCPs) [5]. The MRKPs were constructed based on the Visible Korean Human (VKH) color photographic image data [6], the Korean standard body-shape model of the Size Korea project and the Korean average skeletal models of the Digital Korean project. In addition, the anthropometric dimensions of the MRKPs were matched to the new reference Korean data [4]. The MRKPs include all the source and target regions needed for effective dose calculations, even all the micron-scale regions. To investigate the characteristics of the MRKPs, the organ/tissue masses were compared with the Korean autopsy data [7]. In addition, the chord-length distributions (CLDs) and organ-depth distributions (ODDs) were compared with those of the previous voxel-type reference Korean phantoms.

## 2. Materials and Methods

### *2.1 Reference Korean dataset*

In the present study, the MRKPs were constructed based on the comprehensive reference Korean dataset recently established by Choi *et al.* [4], which includes a total of 133 anthropometric parameters and 58 organ/tissue masses inclusive/exclusive of the blood contents. For the development of MRKPs, 14 anthropometric parameters were selected according to their influence on the dose calculation for external exposures, and applied to develop the MRKPs. Also, the organ masses of MRKPs were matched to organ/tissue masses inclusive of blood contents, assuming that the blood contents are homogenously distributed in organs/tissues.

### *2.2 Development of adult male and female MRKPs*

Most of general organs/tissues of the MRKPs were constructed by directly converting those of color photographic slice images from the VKH project [6] into the high-quality mesh format via surface rendering and refinement procedures [8]. The small and large intestines were exceptionally converted via the Non-Uniform Rational B-Spline (NURBS) conversion process [8]. The skin and skeletal system of the MRKPs were constructed by modifying well-defined polygonal-mesh skin and bone models provided by the Size Korea project (http://sizekorea.kr/) and the Digital Korean project (http://dk.kisti.re.kr/), respectively. For eyeball and lens models, the detailed Korean eye model recently developed by Zhang *et al.* [9] was incorporated into the head of the MRKPs following the same method used for the development of MRCPs [10]. Similarly, the lymphatic nodes were modeled following the same approach used for the development of MRCPs [5]. The models for muscle and blood vessels were manually constructed by referring to the anatomy textbook and the high-quality 3-D models provided by BioDigital Human (http://www.biodigital.com/). Finally, micron-thick target and source regions within alimentary and respiratory tract systems, skin, and urinary bladder were included the MRKPs where a detailed airway model (i.e., bronchi and bronchiole regions) were developed following the method used for the MRCPs [11].

## 3. Results and Discussion

### *3.1 Adult male and female MRKPs*

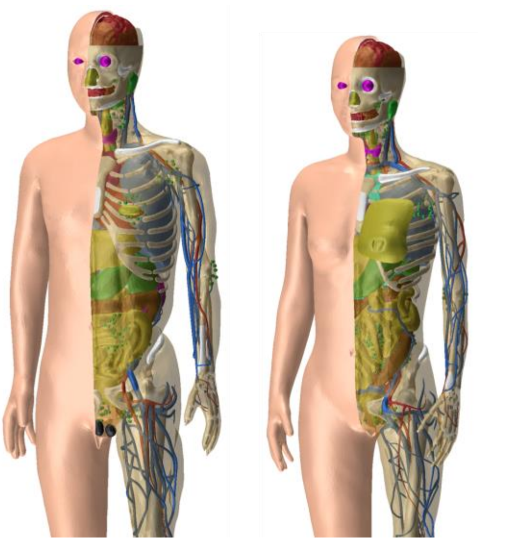

Figure 1. Adult male MRKP (left) and adult female MRKP (right).

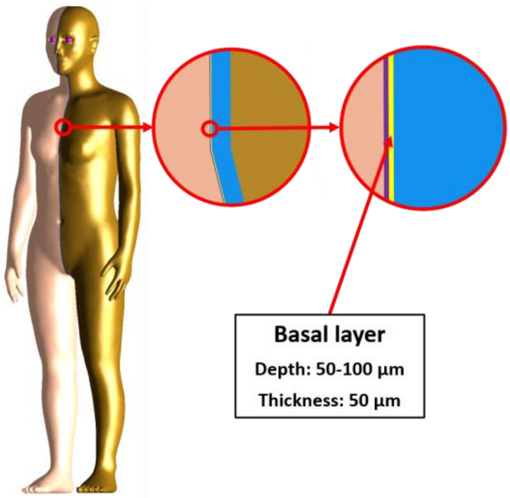


Figure 2. Radiosensitive target region defined in the skin of the female MRKP.

Figure 1 shows the adult male and female MRKPs developed in the present study. The standing heights and total body weights of the MRKPs are consistent with reference Korean values (male: 172 cm and 74 kg, and female: 159 cm and 57 kg). The MRKPs contain 48 organs/tissues with 170 subjects including those required for the effective dose calculation, and their masses were matched to reference Korean values within 0.01% deviation. Besides, the phantoms include the tens-of-micron-thick target and source regions in alimentary and respiratory tract systems, skin, urinary bladder, and eye lens. Figure 2 shows the target region defined in the skin as an example.

### *3.2 Verification of organ masses with Korean autopsy data*

In the present study, the organ masses of the phantoms were compared with Korean autopsy data given in Kim *et al.* [7]. This study measured mean organ masses and their standard deviation for the heart wall, right lung, left lung, liver, right kidney, left kidney, spleen, thyroid, and brain from 526 Korean adult cadavers (369 males and 157 females). Figure 3 shows organ masses of the MRKPs, along with the autopsy data. For the comparison, the organ masses were standardized to have zero mean and unit standard deviation. It can be seen that most of the organ masses are included within one standard deviation bound. The masses of spleen were exceptionally larger than one standard deviation bound of autopsy data, due mainly to the fact that the spleen of the MRKPs fully contains the blood content, whereas blood loss generally occurs during the autopsy procedures. Note that the spleen contains much larger blood content than other organs; that is, the proportion of blood content is ~45% and ~35% for the male and female, respectively.

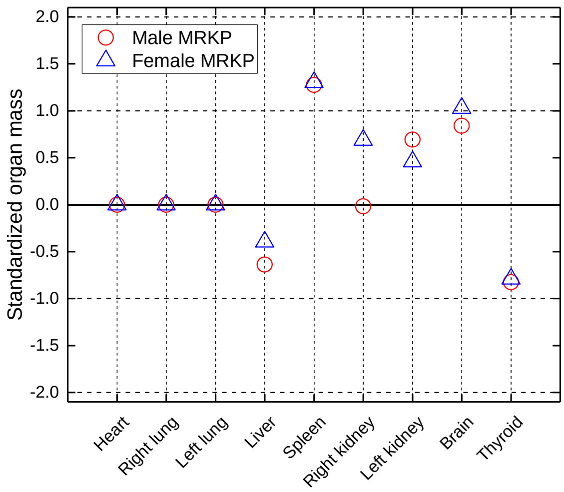


Figure 3. Standardized organ masses of the MRKPs along with Korean autopsy data [8].

### *3.3 Comparison of chord-length distributions and organ-depth distributions*

In the present study, geometrical similarity of the MRKPs with the voxel-type reference phantoms (i.e., HDRK phantoms) was investigated by measuring the two indices (i.e., CLDs and ODDs) of the phantoms, of which importance is already acknowledged in the ICRP [12]. The CLDs represent the distance from source organs to target organs, mainly influencing dose values for internal exposures. On the other hand, the ODDs represent the organ depth from the skin surface, mainly influencing dose values for external exposures.

Tables 1 and 2 show the average values of CLDs and ODDs, respectively. It can be seen that the CLDs of the MRKPs are generally not much different from those of the HDRK phantoms, due to the fact that most of the general organs/tissues for the MRKPs and HDRK phantoms were converted from same tomographic images, that is, VKH images. On the other hand, it can be seen that in general, the ODDs of the MRKPs are different from those of the HDRK phantoms due mainly to the geometrical differences in the skin models used for the development of both phantoms. Note that the Korean

Table 2. Average distances (unit: mm) between ten million randomly sampled point pairs in the liver, lungs, thyroid and urinary bladder contents as source regions and the red bone marrow (RBM), colon, lungs, stomach, breasts, and gonads as target regions.

| Target organs | Source organs | | | | | | | | | | | | | | | |
|---|---|---|---|---|---|---|---|---|---|---|---|---|---|---|---|---|
| | Liver | | | | Lungs | | | | Thyroid | | | | Urinary bladder contents | | | |
| | MRKP | | HDRK | | MRKP | | HDRK | | MRKP | | HDRK | | MRKP | | HDRK | |
| | M | F | M | F | M | F | M | F | M | F | M | F | M | F | M | F |
| RBM | 278.9 | 260.5 | 271.4 | 223.5 | 290.9 | 276.1 | 277.9 | 239.8 | 337.9 | 322.9 | 329.0 | 287.9 | 368.6 | 346.6 | 369.3 | 319.0 |
| Colon | 210.1 | 196.9 | 211.9 | 200.8 | 318.1 | 280.3 | 325.3 | 284.5 | 463.6 | 406.1 | 471.5 | 387.5 | 240.7 | 170.9 | 156.5 | 173.7 |
| Lungs | 175.3 | 150.6 | 182.1 | 144.0 | 143.4 | 127.3 | 147.5 | 107.8 | 199.7 | 176.6 | 195.2 | 142.8 | 524.5 | 397.4 | 440.4 | 420.5 |
| Stomach | 107.1 | 116.1 | 114.0 | 128.0 | 201.4 | 176.5 | 207.1 | 164.2 | 323.7 | 276.8 | 328.1 | 243.4 | 360.8 | 275.6 | 277.5 | 307.7 |
| Breasts | 167.0 | 139.3 | 170.3 | 166.1 | 183.3 | 174.6 | 175.8 | 144.5 | 204.3 | 223.2 | 189.0 | 167.3 | 433.2 | 390.4 | 449.8 | 426.8 |
| Gonads | 320.1 | 334.0 | 394.4 | 290.9 | 435.2 | 424.8 | 519.4 | 379.2 | 590.5 | 563.3 | 673.0 | 489.9 | 42.9 | 42.6 | 91.6 | 60.3 |

M: male, F: female

Table 3. Average depths (unit: mm) of ten million randomly sampled points in the red bone marrow (RBM), colon, lungs, stomach, breasts, and gonad from the skin surface in the front, back, left, and right of the phantoms.

| Target organs | Directions from skin surface | | | | | | | | | | | | | | | |
|---|---|---|---|---|---|---|---|---|---|---|---|---|---|---|---|---|
| | Front | | | | Back | | | | Left | | | | Right | | | |
| | MRKP | | HDRK | | MRKP | | HDRK | | MRKP | | HDRK | | MRKP | | HDRK | |
| | M | F | M | F | M | F | M | F | M | F | M | F | M | F | M | F |
| RBM | 110.5 | 98.5 | 108.3 | 90.5 | 78.2 | 76.1 | 75.8 | 67.7 | 174.0 | 151.3 | 176.7 | 173.4 | 170.5 | 154.1 | 176.0 | 166.2 |
| Colon | 94.5 | 75.8 | 69.6 | 65.5 | 102.3 | 104.9 | 108.4 | 97.0 | 191.2 | 164.9 | 153.2 | 149.1 | 175.7 | 164.7 | 145.3 | 147.5 |
| Lungs | 122.9 | 108.2 | 114.5 | 95.9 | 93.2 | 84.7 | 100.3 | 73.1 | 217.6 | 189.9 | 197.1 | 214.8 | 218.6 | 189.7 | 179.8 | 190.3 |
| Stomach | 77.0 | 54.6 | 66.4 | 57.3 | 143.2 | 148.4 | 165.3 | 132.4 | 132.1 | 94.4 | 111.1 | 77.7 | 177.5 | 154.5 | 167.3 | 166.1 |
| Breasts | 9.1 | 9.7 | 4.1 | 21.1 | 225.9 | 199.9 | 230.0 | 134.2 | 113.2 | 93.8 | 79.6 | 130.8 | 108.0 | 91.8 | 67.5 | 137.2 |
| Gonads | 42.3 | 105.2 | 20.7 | 73.8 | 82.8 | 113.2 | 114.5 | 86.1 | 179.0 | 141.1 | 144.9 | 157.9 | 186.6 | 193.9 | 137.9 | 184.9 |

M: male, F: female

standard body-shape models were used for the skin model of MRKPs, while the VKH images were directly converted for the skin model of HDRK phantoms. From the results, the MRKPs are expected to provide similar dose values to the HDRK phantoms for internal exposures, while providing large differences in dose values for external exposures.

## 4. Conclusion

In the present study, new reference Korean phantoms for adult male and female, named MRKPs, were developed in mesh format to address the limitations of previous reference Korean phantoms. The MRKPs were constructed based on the new reference Korean dataset, and represent all the thin or small organs/tissues, including the micron-thick target and source regions within alimentary and respiratory tract systems, skin, urinary bladder, and eye lens. The characteristic of the MRKPs were then investigated via comparison of organ masses with the Korean autopsy data, and of CLDs and ODDs with the previous voxel-type reference Korean phantoms. Based on the results of the present study, a future study will produce a comprehensive dataset of dose coefficients of Korean adults for external and internal exposures.

## REFERENCES

[1] C. H. Kim, S. H. Choi, J. H. Jeong, C. Lee, and M. S. Chung, HDRK-Man: a whole-body voxel model based on high-resolution color slice images of a Korean adult male cadaver, Phys. Med. Bio., Vol. 53, No. 15, pp. 4093-106, 2008.

[2] Y. S. Yeom, J. H. Jeong, C. H. Kim, M. C. Han, B. K. Ham, K. W. Cho, and S. B. Hwang, HDRK-Woman: whole-body voxel model based on high-resolution color slice images of Korean adult female cadaver, Phys. Med. Bio., Vol. 59, No. 14, pp. 3969-84, 2014.

[3] S. Park, J. K. Lee, J. I. Kim, Y. J. Lee, Y. K. Lim, C. S. Kim, and C. Lee, In vivo organ mass of Korean adults obtained from whole-body magnetic resonance data, Radiat. Prot. Dosim., Vol. 118, No. 3, pp. 275-79, 2005.

[4] C. Choi, Y. S. Yeom, T. T. Nguyen, H. Lee, H. Han, B. Shin, X. Zhang, C. H. Kim, and B. S. Chung, Korean anatomical reference data for adults for use in radiological protection, J. Korean Phys. Soc., Vol. 72, No. 1, pp. 183-91, 2018.

[5] C. H. Kim et al., New mesh-type phantoms and their dosimetric applications, including emergencies, Ann. ICRP, Online: https://doi.org/10.1177/0146645318756231, 2018.

[6] M. S. Chung, J. Y. Kim, W. S. Hwang, and J. S. Park, Visible Korean Human: Another trial for making serially sectioned images, Proc. SPIE, Vol. 4681, pp. 171-84, 2002.

[7] Y. S. Kim, D. I. Kim, S. Y. Cho, M. H. Kim, K. M. Yang, H. Y. Lee, and S. H. Han, Statistical analysis for organ weights in Korean adult autopsies, The Korean J. Anat., Vol. 42, No. 4, pp. 219-24, 2009.

[8] C. H. Kim, J. H. Jeong, W. E. Bolch, K. W. Cho, and S. B. Hwang, A polygon-surface reference Korean male phantom (PSRK-Man) and its direct implementation in Geant4 Monte Carlo simulation, Phys. Med. Biol., Vol. 56, No. 10, pp. 3137-61, 2011.

[9] X. Zhang, H. Han, Y. S. Yeom, T. T. Thang, C. Choi, H. Lee, B. Shin, and C. H. Kim, Development of detailed Korean adult eye model for lens dosimetry, Transaction of KARP Spring Meeting 2018, pp. 172-73, 2018.

[10] T. T. Nguyen, et al., Incorporation of detailed eye model into polygon-mesh versions of ICRP-110 reference phantoms, Phys. Med. Biol., Vol. 60, No. 22, pp. 8695-707, 2015.

[11] H. S. Kim et al., Inclusion of thin target and source regions in alimentary and respiratory tract systems of mesh-type ICRP

adult reference phantoms, Phys. Med. Biol., Vol. 62, No. 6, pp. 2132-52, 2017.
[12] ICRP, Adult reference computational phantoms, ICRP Publication 110, Ann. ICRP 39 (2), 2009.